Brief Report

LYMPHOID NEOPLASIA

CME Article

Tumor cells in light-chain amyloidosis and myeloma show distinct transcriptional rewiring of normal plasma cell development

Daniel Alameda,[1,*] Ibai Goicoechea,[1,2,*] Marco Vicari,[1,*] Elena Arriazu,[1] Alice Nevone,[3] Sara Rodriguez,[1] Marta Lasa,[1] Noemi Puig,[4] Maria Teresa Cedena,[2,5] Diego Alignani,[1,2] Sonia Garate,[1] David Lara-Astiaso,[1] Amaia Vilas-Zornoza,[1,6] Sarai Sarvide,[1] Enrique M. Ocio,[7] Ramon Lecumberri,[1] Alfonso Garcia de Coca,[8] Jorge Labrador,[9] Maria-Esther Gonzalez,[10] Luis Palomera,[11] Mercedes Gironella,[12] Valentin Cabañas,[13] Maria Casanova,[14] Albert Oriol,[15,16] Isabel Krsnik,[17] Albert Perez-Montaña,[18] Javier de la Rubia,[19] Jose-Enrique de la Puerta,[20] Felipe de Arriba,[21] Vito Michele Fazio,[22] Joaquin Martinez-Lopez,[2,5] Juan-Jose Lahuerta,[2,5] Maria-Victoria Mateos,[3] Maria-Dolores Odero,[1] Felipe Prosper,[1,6] Assaf Weiner,[23] Ido Amit,[23] Mario Nuvolone,[3] Jesus F. San Miguel,[1,2] and Bruno Paiva[1,2]

[1]Clinica Universidad de Navarra, Centro de Investigacion Medica Aplicada (CIMA), Instituto de Investigación Sanitaria de Navarra (IDISNA), Pamplona, Spain; [2]Centro de Investigación Biomédica en Red de Oncología (CIBERONC) CB16/12/00369, Pamplona, Spain; [3]Amyloidosis Research and Treatment Center, Foundation IRCCS Policlinico San Matteo, Department of Molecular Medicine, University of Pavia, Pavia, Italy; [4]Centro de Investigación del Cancer, Instituto de Biología Molecular y Celular del Cáncer–Universidad de Salamanca (IBMCC-USAL), Consejo Superior de Investigaciones Científicas (CSIC), Instituto de Investigacion Biomedica de Salamanca (IBSAL), Hospital Universitario de Salamanca, Salamanca, Spain; [5]Centro Nacional de Investigaciones Oncológicas (CNIO), Hospital 12 de Octubre, Universidad Complutense, Madrid, Spain; [6]CIBER-ONC CB16/12/00489, Pamplona, Spain; [7]Hospital Universitario Marqués de Valdecilla (IDIVAL), Universidad de Cantabria, Santander, Spain; [8]Hospital Clínico Universitario de Valladolid, Valladolid, Spain; [9]Hospital Universitario de Burgos, Burgos, Spain; [10]Hospital de Cabueñes, Gijon, Spain; [11]Hospital Clinico Universitario Lozano Blesa, Zaragoza, Spain; [12]Hospital Universitari Vall d'Hebron, Barcelona, Spain; [13]Hospital Clínico Universitario Virgen de la Arrixaca, Murcia, Spain; [14]Hospital Costa del Sol, Marbella, Spain; [15]Institut Català d'Oncologia; [16]Institut Josep Carreras, Hospital Germans Trias i Pujol, Badalona, Spain; [17]Hospital Puerta de Hierro, Madrid, Spain; [18]Hospital Son Espases, Palma, Spain; [19]Hospital Doctor Peset, Valencia, Spain; [20]Hospital de Galdakao, Vizcaya, Spain; [21]Instituto Murciano de Investigación Biosanitaria (IMIB), Hospital Universitario Morales Meseguer, Arrixaca, Spain; [22]UOS Diagnostica Molecolare Ematologica, Campus Bio-Medico University of Rome, Rome, Italy; and [23]Department of Immunology, Weizmann Institute of Science, Rehovot, Israel

KEY POINTS

- Tumor cells express transcriptional programs of both immature and mature stages of normal PC development.

- Survival of patients with AL and MM is inferior when tumor cells express transcriptional programs of more immature normal PC stages.

Although light-chain amyloidosis (AL) and multiple myeloma (MM) are characterized by tumor plasma cell (PC) expansion in bone marrow (BM), their clinical presentation differs. Previous attempts to identify unique pathogenic mechanisms behind such differences were unsuccessful, and no studies have investigated the differentiation stage of tumor PCs in patients with AL and MM. We sought to define a transcriptional atlas of normal PC development in secondary lymphoid organs (SLOs), peripheral blood (PB), and BM for comparison with the transcriptional programs (TPs) of tumor PCs in AL, MM, and monoclonal gammopathy of undetermined significance (MGUS). Based on bulk and single-cell RNA sequencing, we observed 13 TPs during transition of normal PCs throughout SLOs, PB, and BM. We further noted the following: CD39 outperforms CD19 to discriminate newborn from long-lived BM-PCs; tumor PCs expressed the most advantageous TPs of normal PC differentiation; AL shares greater similarity to SLO-PCs whereas MM is transcriptionally closer to PB-PCs and newborn BM-PCs; patients with AL and MM enriched in immature TPs had inferior survival; and protein N-linked glycosylation–related TPs are upregulated in AL. Collectively, we provide a novel resource to understand normal PC development and the transcriptional reorganization of AL and other monoclonal gammopathies.

Medscape Continuing Medical Education online

In support of improving patient care, this activity has been planned and implemented by Medscape, LLC and the American Society of Hematology. Medscape, LLC is jointly accredited by the Accreditation Council for Continuing Medical Education (ACCME), the Accreditation Council for Pharmacy Education (ACPE), and the American Nurses Credentialing Center (ANCC), to provide continuing education for the healthcare team.

JOINTLY ACCREDITED PROVIDER™
INTERPROFESSIONAL CONTINUING EDUCATION

Introduction

Multiple myeloma (MM) and light-chain amyloidosis (AL) are the most common malignant monoclonal gammopathies. Although both present with accumulations of tumor plasma cells (PCs) in bone marrow (BM), AL results from the deposition of misfolded light chains.[1-3] This urged the identification of the unique pathogenic mechanisms in AL. Success in identifying these mechanisms has thus far been limited.[4-7]

Knowledge about the neoplastic transformation of normal PCs remains scarce,[8] particularly when considering the anatomical diversity reflected by their generation in secondary lymphoid organs (SLOs), circulation in peripheral blood (PB), and residence in BM. Thus, we sought to develop a gene-expression atlas of normal PC differentiation throughout SLOs, PB, and BM to compare transcriptional programs (TPs) expressed in tumor PCs of AL vs monoclonal gammopathy of undetermined significance (MGUS) and MM.

Study design

One hundred subjects were studied. Tonsillar and PB-PCs were flow-sorted according to surface heavy-chain immunoglobulin expression, and 5 BM-PC subsets were isolated based on the expression of CD19, CD39, CD56, and CD81, due to their ascribed role in dissecting unique BM-PC differentiation states, from 9 healthy adults (HAs).[9] Tumor PCs from patients with AL (n = 32), MM (n = 32), and MGUS (n = 6) were isolated for RNA sequencing (RNAseq) using fluorescence-activated cell sorting according to patient-specific aberrant phenotypes.[4] We used an RNAseq method optimized for limited cell numbers[10] due to the very small percentages of normal PC subsets in HAs and tumor PCs in AL and

MGUS. Single-cell RNAseq (scRNAseq) was performed in 80 239 PCs from SLOs (n = 3), PB (n = 3), and BM (n = 3) samples from HAs, and BM aspirates from AL (n = 6) and MM (n = 15) patients. The complete methodology is described in supplemental Methods (available on the *Blood* Web site), the study workflow is shown in supplemental Figure 1, and patient characteristics are presented in supplemental Table 1.

Results and discussion

Transition from early to late stages of PC development includes cessation of the cell cycle and activation of antiapoptotic genes.[11-13] Thus, prolonged survival of long-lived normal PCs could be an intrinsic advantage before their neoplastic transformation, whereas blocked proliferation after exiting SLOs would pose a challenge to their clonal expansion. Yet, precise knowledge about the TPs expressed by tumor PCs in relation to normal PC development remains unknown. Hence, we first displayed a 3-dimensional principal component analysis of normal and tumor PC gene expression (Figure 1A), which exposed the presence of 13 TPs during the transition of normal PCs throughout SLOs, PB, and BM (Figure 1B), and uncovered that tumor PCs express TPs linked to various stages of normal PC differentiation (Figure 1C).

As expected, TPs related to germinal center formation and B-cell activation/proliferation were turned off once normal PCs egressed from SLOs (TP-3 and TP-4). By contrast, genes related to NF-κB, among others, in TP-9 became active from the moment PCs left SLOs. The transition from PB- into BM-PCs was characterized by differential expression of genes related to protein secretion (TP-10), whereas newborn and long-lived BM-PC subsets differed on the expression of genes associated with proliferation (TP-5) and survival
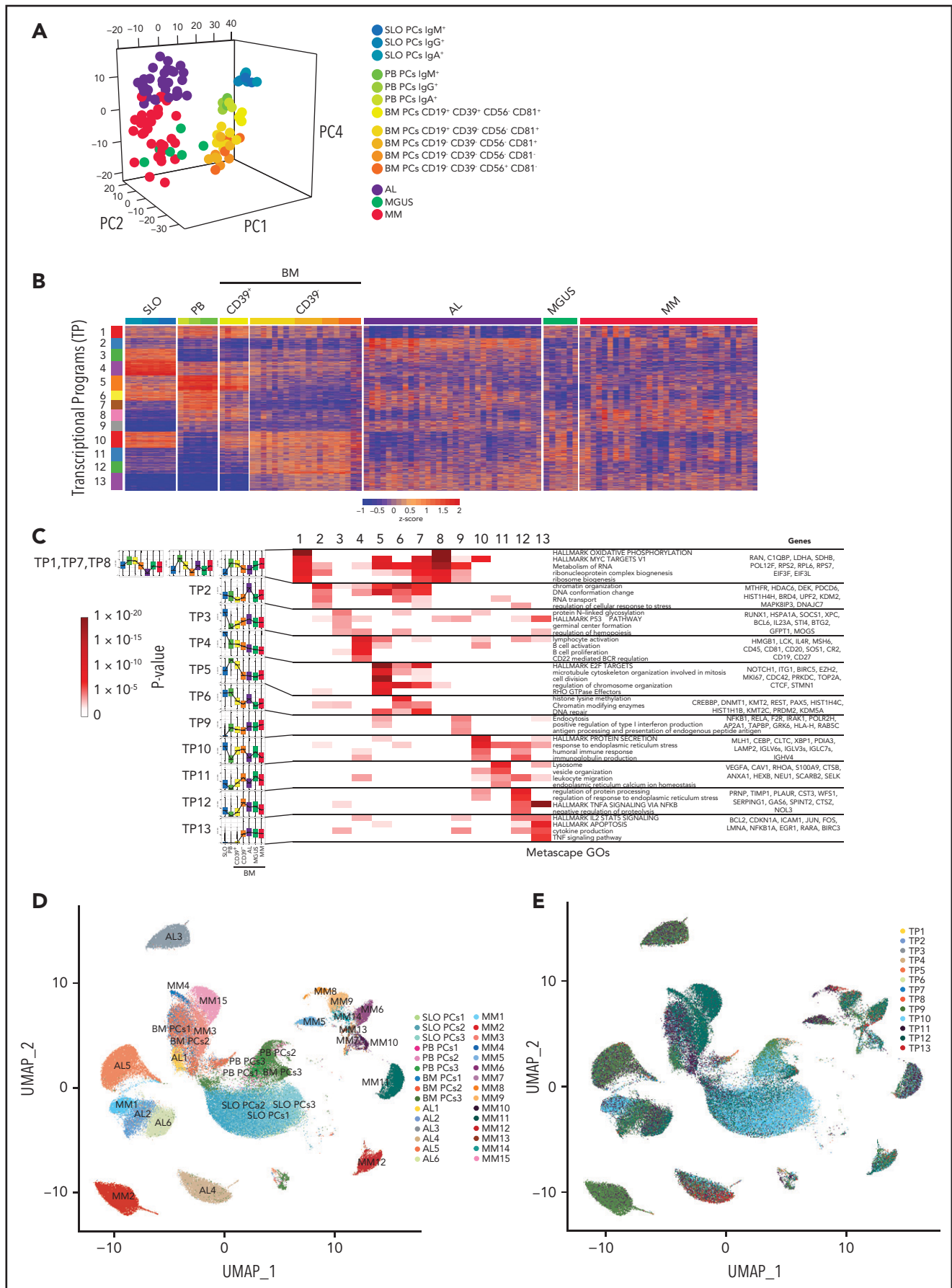
ALAMEDA et al

Figure 1.

(TP-13). This transcriptional atlas of normal PC differentiation may contribute to further insights on genes involved in the generation of antibody-secreting cells and maturation into long-lived BM-PCs.[13] For example, we observed that CD39 outperforms CD19 as a marker to discriminate newborn (CD39^{+}) from long-lived (CD39^{−}) normal BM-PCs (Figure 1B; supplemental Figure 2).

There are divergent opinions about the anatomical origin of monoclonal gammopathies in accordance with different concepts of disease pathogenesis; namely an antibody-secreting cell that originates from post–germinal center B cells in SLOs and can be detected in PB vs long-lived PCs in the BM.[14-19] Here, we unraveled that tumor PCs from AL, MM, and MGUS patients express TPs from more immature SLOs, PB, and newborn PCs (eg, *MYC* activation in TP-7, TP-8) together with TPs from long-lived BM-PCs (eg, survival in TP-13). By contrast, reduced protein secretion (eg, TP-10) and regulation of response to endoplasmic reticulum stress (eg, TP-12) emerged as hallmarks of the neoplastic transformation from normal, long-lived BM-PCs into tumor PCs.

Based on the nonsuperimposable distribution of tumor PCs from AL, MM, and MGUS patients throughout the various stages of normal PC development (principal component 4 in Figure 1A), we decided to determine gene-expression correlation levels between each TP in the multiple normal PC subsets vs tumor PCs from each disease (supplemental Figure 3A). As such, the TPs that better defined each normal PC subset were identified, and their relative weight was measured in tumor PCs to unbiasedly identify their closest normal PC counterpart (supplemental Figure 3B). Surprisingly, we found that whereas TPs from SLOs, PB, and newborn and long-lived BM-PCs were equally distributed in MGUS, there was predominant expression of TPs from SLO-PCs in AL and TPs from PB- plus newborn BM-PCs in MM (supplemental Figure 3C).

We then used scRNAseq to investigate whether these TPs were homogeneously (vs heterogeneously) expressed in individual normal and tumor PCs (Figure 1D). As expected, normal PCs clustered according to their differentiation. Some patients also clustered, which could be partially explained by the proliferative stage of tumor PCs (supplemental Figure 4) and, to a lesser extent, *IGH* translocations (supplemental Figure 5). Furthermore, we observed that, whereas all AL patients had a predominant TP expressed by a majority of tumor PCs (ie, TP-9, TP-11, and TP-12; Figure 1E; supplemental Figure 6A), there was considerable single-cell diversity and most TPs were detectable in smaller percentages of tumor PCs (supplemental Figure 6A-B). These

findings build upon recent concepts about the evolutionary trade-offs of cancer hallmarks.[20,21] Thus, rather than tumors being forced to select 1 biological function (eg, proliferation, survival, invasion, etc), singular PC subsets would be specialized in one or another task, and subset predominance in response to stimuli (eg, hypoxia) would dictate the tumor phenotype in a given moment.

Because previous studies in MM have shown an association between the differentiation stage of tumor PCs and patient outcome,[9] we investigated whether the same applied to AL. First, we defined a normalized enrichment score (NES) based on the transcriptional profile of SLO-PCs, PB-PCs plus newborn BM-PCs and long-lived BM-PCs (supplemental Figure 7). As expected, the various normal PC subsets from SLOs, PB, and BM displayed the highest corresponding NES, whereas tumor PCs from AL and MM patients showed higher NES values related to the transcriptional profile of SLO-PCs and PB-PCs/newborn BM-PCs, respectively (Figure 2A). Although the number of patients precludes definitive conclusions, AL patients with tumor PCs displaying higher NES values corresponding to normal SLO-PCs had significantly inferior progression-free survival (Figure 2B-C). Similarly, we found that, in a larger series of patients with MM enrolled in CoMMpass, those displaying high NES values corresponding to PB-PCs/newborn BM-PCs had significantly poorer outcome (Figure 2D-E and supplemental Figure 8, in which *MKI67* was removed).

This is the first integrated bulk and single-cell analysis of the transcriptional programs of anatomically different normal PC subsets vs tumor PCs in AL, MM, and MGUS. Our results unveiled shared and exclusive transcriptional states between normal and tumor PCs, together with unique differences in tumor PCs from patients with AL, MM, and MGUS (supplemental Figure 9). Indeed, there were 720 genes differentially expressed in AL vs MM and MGUS (supplemental Table 2). It could be hypothesized that the greater similarity between MGUS and MM is because most MGUS progress into MM and not AL. Larger studies are needed to confirm this, and that specific cytogenetic abnormalities have no impact in transcriptional differences between AL vs MGUS/MM (supplemental Figure 10).

Two-thirds of genes overexpressed in AL vs MM/MGUS belonged to TP-2, TP-3, and TP-6 (213 of 335; 64%). These are linked to chromatin organization and protein N-linked glycosylation, which becomes downregulated as normal PCs egress from SLOs (Figure 1B-C). Interestingly, there is a fourfold higher rate of *N*-glycosylation in light chains from patients with AL vs other PC disorders,[22]

Figure 1. Transcriptional atlas of normal PC development and neoplastic transformation. Data were normalized with RUVSeq, and differential expression of genes was analyzed with Deseq2 or masigpro, followed by k-means clustering in R. (A) Tridimensional principal component analysis of gene-expression data based on the top 500 variable genes. Normal PCs were isolated by fluorescence-activated cell sorting (FACS) from SLOs (ie, tonsils, SLO) and PB according to immunoglobulin heavy-chain isotypes, as well as from BM samples of healthy adults according to differential expression of CD19, CD39, CD56, and CD81. Tumor PCs were isolated by FACS from BM samples of patients with AL (n = 32), MGUS (n = 6), and MM (n = 32). (B) Heat map of gene expression in normal PC subsets (after merging SLO- and PB-PCs with immunoglobulin M [IgM], IgG, and IgA isotypes as well as all CD39^{−} BM-PCs due to overlapping profiles) and tumor PCs from AL, MGUS, and MM patients, based on a total of 2200 genes selected by their differential expression in normal SLO-PCs, PB-PCs, and CD39^{+} and CD39^{−} BM-PCs plus 720 genes differentially expressed in tumor PCs from AL, MGUS, and MM patients. TPs were defined by semisupervised k-means clustering (k = 13), and gene expression is represented with a row z score. (C) Functional enrichment heat map based on top nonredundant biological functions (ie, gene ontology [GO]) (*P* < .05) per TP determined with Metascape. TP1, TP7, TP8 shared the same top biological functions and were grouped. Color intensity is proportional to the significance level. Box plots from left to right represent gene-expression levels in normal SLO-PCs, PB-PCs, and CD39^{+} and CD39^{−} BM-PCs as well as tumor PCs from AL, MGUS, and MM patients. The most significant deregulated genes are shown at the right end of the graphical representation. (D) Uniform manifold approximation and projection (UMAP) of 142 778 individual PCs isolated by FACS from healthy adults; SLOs (n = 3), PB (n = 3), and BM (n = 3) and from patients with AL (n = 6) and MM (n = 15). (E) Single normal BM-PCs and tumor PCs were colored according to the TPs identified in panel C, based on the expression level of the most significant genes defining each TP. We used the Seurat R package[24] for data integration and clustering.
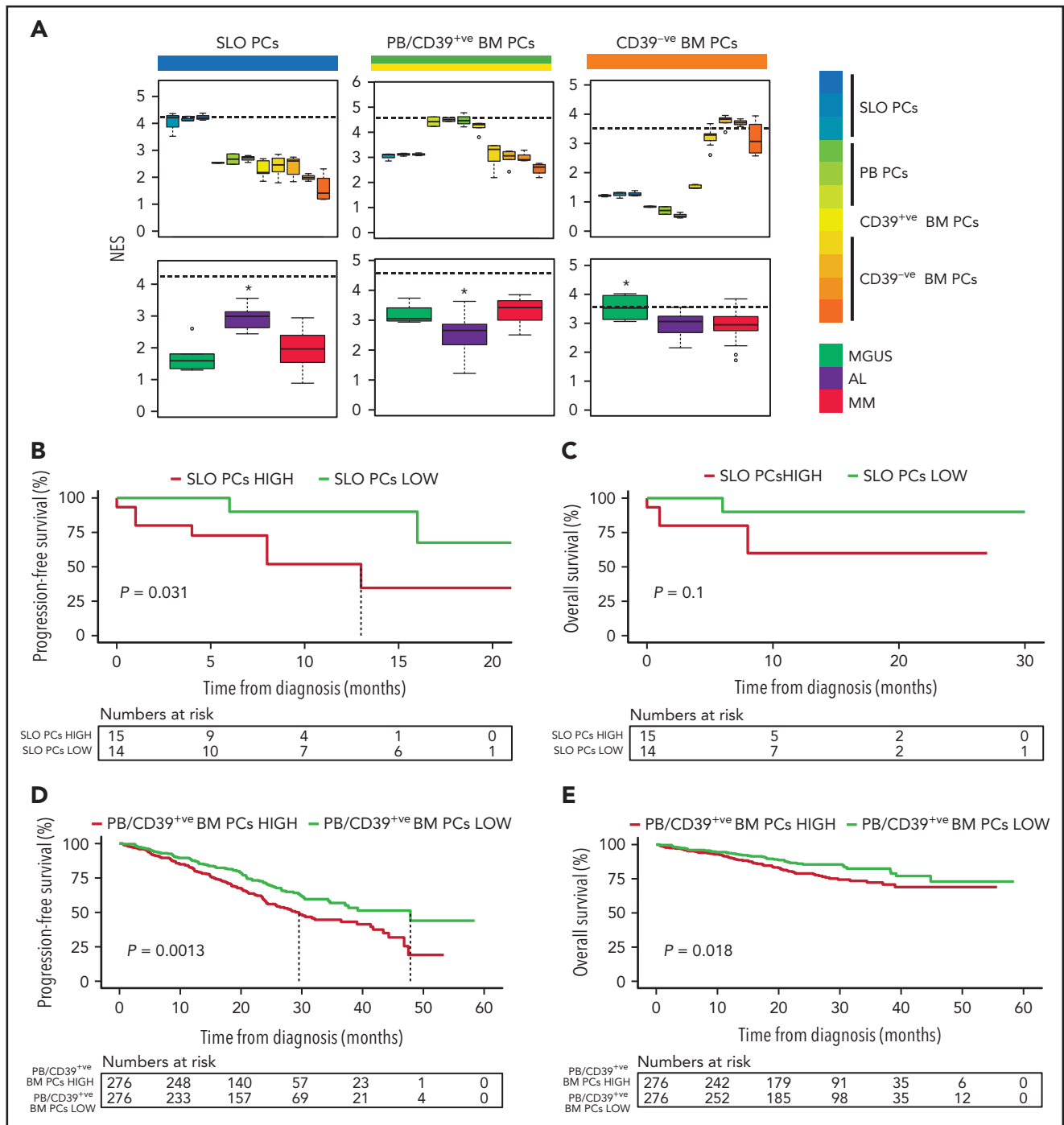
Figure 2. Impact of tumor gene expression in the survival of patients with AL and MM according to the resemblance with normal PC counterparts. (A) NES values based on the transcriptional profile of SLOs (ie, tonsils, SLO), PB, CD39$^+$ (CD39^{+ve}), and CD39$^-$ (CD39^{-ve}) BM normal PCs, measured in these as well as in tumor PCs from patients with AL (n = 32), MGUS (n = 6), and MM (n = 32). The dashed line marks the median NES of the corresponding normal PC subset. *$P < .05$. (B-C) Progression-free and overall survival of patients with AL (n = 29) according to low vs high NES values corresponding to normal SLO-PCs (red, NES value above the median; green, NES values below the median). (D-E) Progression-free and overall survival of patients with MM (n = 552) according to low vs high NES values corresponding to normal PB-PCs and CD39$^+$ BM-PCs (red, NES values above the median; green, NES values below the median).

although we could not confirm in vitro that knockdown of *NAGK* and *MGAT2* reduced *N*-glycosylation of light chains produced by KJON cells (supplemental Figure 11).

More than one-half of genes underexpressed in AL vs MM/MGUS belonged to TP-1 and TP-8 (223 of 385; 58%), which

are associated with oxidative phosphorylation, *MYC*, or ribosome biogenesis that becomes upregulated as normal PCs egress from SLOs (Figure 1B-C). These findings are consistent with previous observations about impaired ribosome machinery in AL.[23] Thus, our results could potentially shed new light into the different clinical presentation of AL.

Footnotes

REFERENCES

1. Gertz MA. Immunoglobulin light chain amyloidosis: 2020 update on diagnosis, prognosis, and treatment. *Am J Hematol.* 2020;95(7):848-860.

2. Rajkumar SV. Multiple myeloma: 2020 update on diagnosis, risk-stratification and management [published correction appears in *Am J Hematol.* 2020;95(11):1444]. *Am J Hematol.* 2020;95(5):548-567.

3. Merlini G, Dispenzieri A, Sanchorawala V, et al. Systemic immunoglobulin light chain amyloidosis. *Nat Rev Dis Primers.* 2018;4(1):38.

4. Paiva B, Martinez-Lopez J, Corchete LA, et al. Phenotypic, transcriptomic, and genomic features of clonal plasma cells in light-chain amyloidosis. *Blood.* 2016;127(24):3035-3039.

5. Cuenca I, Alameda D, Sanchez-Vega B, et al. Immunogenetic characterization of clonal plasma cells in systemic light-chain amyloidosis. *Leukemia.* 2021;35(1):245-249.

6. Puig N, Paiva B, Lasa M, et al. Flow cytometry for fast screening and automated risk assessment in systemic light-chain amyloidosis. *Leukemia.* 2019;33(5):1256-1267.

7. Boyle EM, Ashby C, Wardell CP, et al. The genomic landscape of plasma cells in systemic light chain amyloidosis. *Blood.* 2018;132(26):2775-2777.

8. Davies FE, Dring AM, Li C, et al. Insights into the multistep transformation of MGUS to myeloma using microarray expression analysis. *Blood.* 2003;102(13):4504-4511.

9. Paiva B, Puig N, Cedena MT, et al. Differentiation stage of myeloma plasma cells: biological and clinical significance. *Leukemia.* 2017;31(2):382-392.

10. Jaitin DA, Kenigsberg E, Keren-Shaul H, et al. Massively parallel single-cell RNA-seq for marker-free decomposition of tissues into cell types. *Science.* 2014;343(6172):776-779.

11. Shapiro-Shelef M, Calame K. Regulation of plasma-cell development. *Nat Rev Immunol.* 2005;5(3):230-242.

12. Radbruch A, Muehlinghaus G, Luger EO, et al. Competence and competition: the challenge of becoming a long-lived plasma cell. *Nat Rev Immunol.* 2006;6(10):741-750.

13. Nguyen DC, Joyner CJ, Sanz I, Lee FE. Factors affecting early antibody secreting cell maturation into long-lived plasma cells. *Front Immunol.* 2019;10:2138.

14. Huff CA, Matsui W. Multiple myeloma cancer stem cells. *J Clin Oncol.* 2008;26(17):2895-2900.

15. Abe M, Harada T, Matsumoto T. Concise review: Defining and targeting myeloma stem cell-like cells. *Stem Cells.* 2014;32(5):1067-1073.

16. Matsui W, Wang Q, Barber JP, et al. Clonogenic multiple myeloma progenitors, stem cell properties, and drug resistance. *Cancer Res.* 2008;68(1):190-197.

17. Matsui W, Huff CA, Wang Q, et al. Characterization of clonogenic multiple myeloma cells. *Blood.* 2004;103(6):2332-2336.

18. Leung-Hagesteijn C, Erdmann N, Cheung G, et al. Xbp1s-negative tumor B cells and pre-plasmablasts mediate therapeutic proteasome inhibitor resistance in multiple myeloma [published correction appears in *Cancer Cell.* 2015;28(4):541-542]. *Cancer Cell.* 2013;24(3):289-304.

19. Thiago LS, Perez-Andres M, Balanzategui A, et al. Circulating clonotypic B cells in multiple myeloma and monoclonal gammopathy of

undetermined significance. *Haematologica.* 2014;99(1):155-162.

20. Hausser J, Alon U. Tumour heterogeneity and the evolutionary trade-offs of cancer. *Nat Rev Cancer.* 2020;20(4):247-257.

21. Hanahan D, Weinberg RA. Hallmarks of cancer: the next generation. *Cell.* 2011; 144(5):646-674.

22. Kumar S, Murray D, Dasari S, et al. Assay to rapidly screen for immunoglobulin light chain glycosylation: a potential path to earlier AL diagnosis for a subset of patients [published correction appears in *Leukemia.* 2019;33(4):1060]. *Leukemia.* 2019;33(1): 254-257.

23. Kryukov F, Kryukova E, Brozova L, et al. Does AL amyloidosis have a unique genomic profile? Gene expression profiling meta-analysis and literature overview. *Gene.* 2016;591(2): 490-498.

24. Butler A, Hoffman P, Smibert P, Papalexi E, Satija R. Integrating single-cell transcriptomic data across different conditions, technologies, and species. *Nat Biotechnol.* 2018;36(5): 411-420.